

Three Families of Nonlinear Subdivision Schemes

Nira Dyn

School of Mathematical Sciences, Tel-Aviv University, Israel

Abstract

Three families of nonlinear subdivision schemes, derived from linear schemes, are reviewed. The nonlinearity is introduced into the linear schemes by adapting the schemes to the data. The first family, derived from the four-point interpolatory linear subdivision scheme, consists of geometrically controlled schemes, which are either shape preserving or artifact-free. The second family of schemes is designed for the functional setting, to be used in constructions of multiscale representations of piecewise smooth functions. The schemes are extensions of the Dubuc-Deslauriers 2N-point interpolatory schemes, with the classical local interpolation replaced by ENO or WENO local interpolation. The third family consists of subdivision schemes on smooth manifolds. These schemes are derived from converging linear schemes, represented in terms of repeated binary averages. The analysis of the nonlinear schemes is done either by proximity to the linear schemes from which they are derived, or by methods adapted from methods for linear schemes.

Key words: linear and nonlinear subdivision scheme, adaptive tension parameter, convexity preserving scheme, ENO interpolation, data dependent scheme, repeated binary averages, refinement on a manifold, geodesics, projection onto a manifold

2000 MSC: 65D05, 65D07, 65D10, 65D15, 65D17, 65U05, 65U07

Email address: niradyn@post.tau.ac.il (Nira Dyn).

1. Introduction

Linear subdivision schemes are an important tool for the design and generation of curves and surfaces in geometric modelling. A further motivation for the study of subdivision schemes is their close relation to multiresolution analysis and wavelets (see e.g. [4]).

Linear subdivision schemes have been investigated for the last 20 years. Tools for analyzing their convergence and smoothness are now available. Yet, linear schemes have many limitations being independent of the data upon which they operate.

In this paper we review three families of nonlinear subdivision schemes, handling three different settings in which linear schemes fail. The construction of the nonlinear schemes is closely related to linear schemes and so is their analysis.

The first setting is a geometric setting of control polygons in 2D or 3D. The performance of linear subdivision schemes on initial control polygons with edges of comparable lengths is known to be satisfactory. But curves generated by linear schemes from control polygons with edges of significantly different lengths tend to have artifacts, such as self intersections and inflection points which do not correspond to the shape of the initial control polygon. We present a construction of a nonlinear scheme which alleviates the artifacts. The construction is based on the linear 4-point interpolatory scheme with a tension parameter. The nonlinearity is introduced by choosing the tension parameter adaptively for each inserted point, according to the geometry of the relevant local control polygon, which consists of the four points involved in the definition of the inserted point. The idea of adaptive tension parameter is used also for obtaining shape preserving schemes in 2D, such as convexity-preserving schemes. These two types of geometrically controlled 4-point schemes are reviewed in Section 2, following the paper [11]. A different construction of a nonlinear four-point scheme, which is circle-preserving, is studied in [16].

The second setting is a functional setting with data sampled from a piecewise smooth function [2]. The nonlinear subdivision schemes are data dependent, and are extensions of the Dubuc-Deslauries $2N$ -point interpolatory schemes. The nonlinearity is introduced by using the ENO (Essentially Non Oscillatory) idea of choosing a stencil for local interpolation, among several possible ones, according to the data. The choice of the stencil for estimating an inserted point aims at stencils which consist of points all from the same smoothness region. In order to obtain “stable schemes”, namely schemes which depend continuously on the data, the WENO (Weighted ENO) idea is used instead of the ENO idea. Section 3 reviews mainly the special case corresponding to the 4-point scheme ($N = 2$).

The third setting is that of curves on smooth manifolds. Converging linear schemes are so changed to generate control points on the manifold at each refinement level. The analysis of the resulting nonlinear schemes is done by their proximity to the linear schemes from which they are derived, and from properties of the linear schemes obtained by known methods (see e.g. [6]). We discuss two general constructions of nonlinear schemes from linear schemes. The material is taken mainly from [17] and partially from [18], and is presented in Section 4. Similar constructions and results

are presented in [17] and [18] for subdivision schemes in certain matrix groups and in certain Lie groups. This material is not reviewed here.

There are not many works in the literature on nonlinear subdivision schemes on manifolds. Analogous schemes to quadratic B-spline schemes on manifolds are studied in [12], [13]. A general approach to the construction of nonlinear schemes for manifold data from linear schemes is developed in [15]. The construction is different from those presented in Section 4. The schemes in [15] are used for multiscale representations of manifold-valued data.

The idea of analyzing subdivision schemes, related to linear ones, by proximity is not new. In [7] non-stationary linear schemes are analyzed by their proximity to stationary linear schemes. Here we mention two other types of nonlinear schemes that were analyzed in relation to linear ones. The first type is that of the “median interpolating” subdivision schemes and their extensions [19], [20], [14], where the nonlinearity is rather weak. The second type is that of the “normal curves” [5].

2. Geometrically Controlled 4-point Interpolatory Schemes

In this section we present nonlinear versions of the linear 4-point interpolatory scheme [8], which adapt the tension parameter to the geometry of the control points. It is well known that the linear 4-point scheme with the refinement rules

$$P_{2j}^{k+1} = P_j^k, \quad P_{2j+1}^{k+1} = -w(P_{j-1}^k + P_{j+2}^k) + (\frac{1}{2} + w)(P_j^k + P_{j+1}^k), \quad (1)$$

where w is a fixed tension parameter, generates a good curve from initial control points $\{P_j^0\}$, if the edges of the control polygon, $e_j^0 = P_{j+1}^0 - P_j^0$, have comparable length. The generated curve is C^1 for $w \in (0, w^*)$, where the value of w^* is not known, but it is known that $w^* < \frac{1}{8}$ [8].

In case of a control polygon with edges of significantly different lengths, the curve generated by (1) has artifacts such as self-intersections and inflection points which are not seen in the initial control polygon (see Fig. 1).

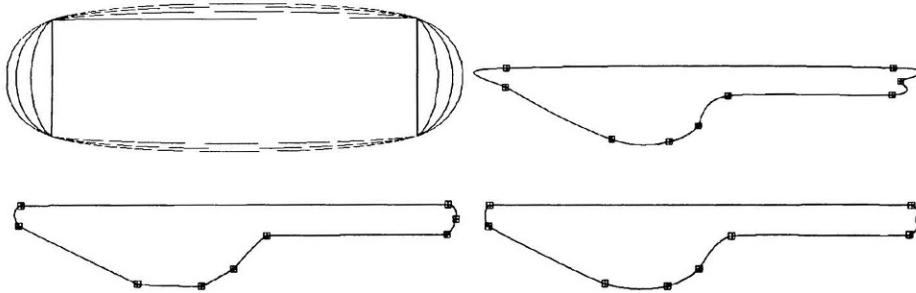


Fig. 1. Curves generated by the linear 4-point scheme: (upper left) the effect of different tension parameters, (upper right) artifacts in the curve generated with $w = \frac{1}{16}$, (lower left) artifact-free but visually non-smooth curve generated with $w = 0.01$. (Lower right) artifact-free and visually smooth curve generated in a nonlinear way with adaptive tension parameters.

To overcome this problem we developed in [11] nonlinear 4-point interpolatory schemes of the form (1) but with w chosen adaptively according to the geometry of the control polygon of the 4 points in (1).

Writing the insertion rule for P_{2j+1}^{k+1} in (1) in terms of the edges $e_j^k = P_{j+1}^k - P_j^k$, and relating the inserted point P_{2j+1}^{k+1} to the edge e_j^k , we get

$$P_{e_j^k} = M_{e_j^k} + w_{e_j^k}(e_{j-1}^k - e_{j+1}^k) \quad (2)$$

with $M_{e_j^k}$ the midpoint of e_j^k and $w_{e_j^k}$ the adaptive tension parameter for the refinement of e_j^k . Defining $d_{e_j^k} = w_{e_j^k}(e_{j-1}^k - e_{j+1}^k)$ as the displacement from $M_{e_j^k}$, we control its size by choosing $w_{e_j^k}$ according to a chosen geometrical criterion.

Here we review two such criteria. More criteria can be found in [11].

2.1. Displacement-safe schemes

In this family of schemes, $w_{e_j^k}$ is chosen so that

$$\|d_{e_j^k}\| < \frac{1}{2}\|e_j^k\| \quad \text{for } \|e_j^k\| > 0. \quad (3)$$

This choice guarantees that the inserted control point $P_{e_j^k}$ is different from the boundary points of the edge e_j^k and that the length of each of the two edges replacing e_j^k is less than the length of e_j^k , namely

$$\begin{aligned} \|e_{2j}^{k+1}\| &= \|P_{e_j^k} - P_j^k\| < \|e_j^k\| \\ \|e_{2j+1}^{k+1}\| &= \|P_{j+1}^k - P_{e_j^k}\| < \|e_j^k\| \end{aligned}$$

There are many ways to impose (3). We restrict the adaptive tension parameter $w_{e_j^k}$ to the interval $(0, \frac{1}{16}]$, so that a tension close to 1/16 is assigned to “regular stencils” e.g. stencils of four points with three edges of almost equal length. The less regular the stencil, the closer to zero is the tension parameter assigned to it. These heuristics are based on these observations about the linear 4-point scheme:

- This scheme generates “good” curves when applied to control polygons with edges of comparable length.
- This scheme generates curves which become smoother, the closer the tension parameter is to 1/16.
- For initial control polygons with edges of significantly different lengths, this scheme generates curves which preserve the shape of the initial control polygons, only for very small values of the tension parameters. (Recall that the control polygon itself corresponds to the generated curve with zero tension parameter.)

A “natural” choice of an adaptive tension parameter obeying (3) is

$$w_{e_j^k} = \min \left\{ \frac{1}{16}, c \frac{\|e_j^k\|}{\|e_{j-1}^k - e_{j+1}^k\|} \right\}, \quad \text{with a fixed } c \in (0, \frac{1}{2}). \quad (4)$$

Furthermore, we restrict c to the interval $[\frac{1}{8}, \frac{1}{2})$ to guarantee that $w_{e_j^k} = \frac{1}{16}$ for stencils with $\|e_{j-1}^k\| = \|e_j^k\| = \|e_{j+1}^k\|$. Indeed in this case, $\|e_{j-1}^k - e_{j+1}^k\| = 2 \sin \frac{\theta}{2} \|e_j^k\|$, with $\theta, 0 < \theta \leq \pi$, the angle between the two vectors e_{j-1}^k, e_{j+1}^k . Thus $\|e_j^k\| / \|e_{j-1}^k - e_{j+1}^k\| = (2 \sin \frac{\theta}{2})^{-1} \geq \frac{1}{2}$, and if $c \geq \frac{1}{8}$ then the minimum in (4) is $\frac{1}{16}$. The choice (4) defines irregular stencils (corresponding to small $w_{e_j^k}$) as those with $\|e_j^k\|$ much smaller than at least one of $\|e_{j-1}^k\|, \|e_{j+1}^k\|$, and such that when these two edges are of comparable length, the angle between them is not close to zero.

Moreover, for $\|e_j^k\| = 0$ we take $w_{e_j^k} = 0$, and then $P_{2j+1}^{k+1} = P_j^k = P_{j+1}^k$. Thus two repeated control points in the initial control polygon generate a corner in the limit curve, while due to (3), new repeated control points are not generated during the refinement process.

This feature of the displacement-safe scheme allows to generate piecewise smooth curves from initial control polygons with some repeated consecutive control points.

The convergence of the displacement-safe scheme, namely the convergence of the sequence of polygonal lines through the control points at each refinement level, is a consequence of the following result on the 4-point scheme with variable tension parameters, applied to scalar data [10].

Theorem 1. *The 4-point scheme with variable tension parameters has the refinement rules*

$$f_{2j}^{k+1} = f_j^k, \quad f_{2j+1}^{k+1} = \left(\frac{1}{2} + w_j^k \right) (f_j^k + f_{j+1}^k) - w_j^k (f_{j-1}^k + f_{j+2}^k). \quad (5)$$

It converges to continuous limit functions, if there is an $\varepsilon > 0$ such that $w_j^k \in [0, \frac{1}{8} - \varepsilon]$ for all (j, k) . The scheme generates C^1 limit functions, if for all (j, k) , $w_j^k \in [\varepsilon, \frac{1}{8} - \varepsilon]$, for some $\varepsilon > 0$.

The choice (4) of the adaptive tension parameters guarantees that for all (j, k) , $w_{e_j^k} \in [0, \frac{1}{16}]$ and therefore by Theorem 1 applied to the components of the curve, the displacement-safe scheme defined by (4) converges and generates continuous curves. Yet we cannot conclude from Theorem 1 that the limit curves generated by this scheme are C^1 , since the tension parameters used, during the subdivision process, are not bounded away from zero.

Nevertheless, our many simulations indicate that the curves generated by the displacement-safe scheme, based on (4), are C^1 (see Fig. 4).

If indeed these curves are C^1 , then the displacement safe scheme based on (4) does not generate corners in the limit, and the resulting curves are piecewise smooth with corners only at repeated control points of the initial control polygon.

2.2. Convexity-preserving schemes in the plane

A shape property of planar control polygons, which is important to have in the curves generated by subdivision, is convexity. This can be achieved by a proper choice of the adaptive tension parameters.

To present this choice, we first introduce some local geometrical notions.

An edge such that its two neighboring edges are in the same half-plane, determined by the line through the edge, is termed a “convex edge”.

An edge which is on the same line as one of its neighboring edges is termed a “straight edge”.

A line through a control point, such that the two edges meeting at the control point are on the same side of the line, is termed a “convex tangent”. A “straight tangent” at a control point is a line through one of the edges emanating from the point.

A polygon consisting of convex and straight edges is termed a “convex polygon”. It is a “strictly convex polygon” if all its edges are convex. In Fig. 2 three examples of strictly convex polygons are given.

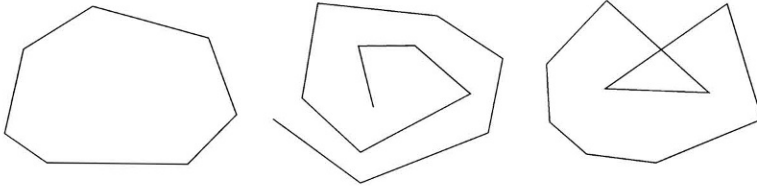


Fig. 2. Convex polygons: (left) closed, (middle) open, (right) self-intersecting.

The algorithm we present refines convex (strictly convex) control polygons into convex (strictly convex) control polygons. The construction of the inserted point $P_{e_j^k}$ is a geometric construction, which determines the displacement vector $w_{e_j^k}(e_{j-1}^k - e_{j+1}^k)$ rather than $w_{e_j^k}$ directly as in (4).

As a first step in the construction, at each control point from which at least one convex edge emanates, a convex tangent is constructed. At all other control points a straight tangent is constructed, coinciding with one of the straight edges meeting at the control point. We denote the tangent at P_j^k by t_j^k .

In case of a straight edge e_j^k , $P_{e_j^k} = M_{e_j^k}$. For a convex edge e_j^k , the construction of $P_{e_j^k}$ is illustrated schematically in Fig. 3. In this case, the tangents t_j^k and t_{j+1}^k together with e_j^k determine a triangle, $T_{e_j^k}$. By construction, the triangle $T_{e_j^k}$ and the edges e_{j-1}^k, e_{j+1}^k are on two different sides of the line through e_j^k .

The line from $M_{e_j^k}$ along the direction $e_{j-1}^k - e_{j+1}^k$ has a segment, $I_{e_j^k}$, inside $T_{e_j^k}$. Let $L_{e_j^k}$ denote the length of $I_{e_j^k}$. The point $P_{e_j^k}$ is chosen on $I_{e_j^k}$ so that

$$\|P_{e_j^k} - M_{e_j^k}\| = \min \left\{ \frac{1}{16} \|e_{j-1}^k - e_{j+1}^k\|, CL_{e_j^k} \right\},$$

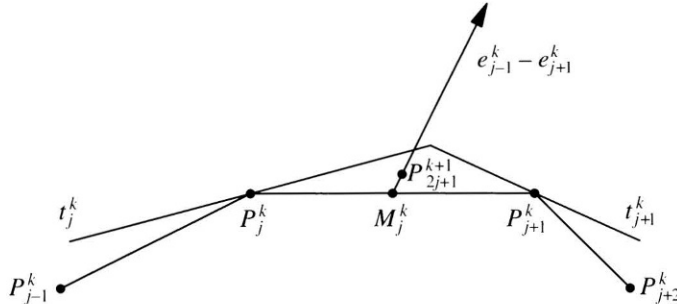


Fig. 3. Construction of an inserted point for a convex edge.

with a fixed C , satisfying $\frac{1}{2} < C < 1$. This choice guarantees that $0 < w_{e_j^k} \leq \frac{1}{16}$ and that the refined control polygon $\{P_j^{k+1}\}$ with

$$P_{2j}^{k+1} = P_j^k, \quad P_{2j+1}^{k+1} = P_{e_j^k},$$

is convex (strictly convex) if the control polygon $\{P_j^k\}$ is (see [11]).

This construction of refined control polygons when repeated generates a sequence of convex (strictly convex) polygons from an initial convex (strictly convex) polygon. It is proved in [11] that the limit of this sequence is a continuous convex (strictly convex) curve. Moreover, it is proved that the curve between two consecutive initial control points is either a line segment when the edge connecting these two points in the initial control polygon is straight, or otherwise a strictly convex curve.

Note that the subdivision scheme is interpolatory and that P_{2j+1}^{k+1} depends on the points $P_{j-1}^k, P_j^k, P_{j+1}^k, P_{j+2}^k$ as in the linear 4-point scheme.

The convex tangents in this construction can be chosen in different ways. A natural choice of such a tangent is

$$t_j^k = P_{j+1}^k - P_{j-1}^k = e_j^k + e_{j-1}^k.$$

This choice was tested in many numerical experiments, and was found superior to other choices.

In Fig. 4, the performance of the convexity-preserving scheme is compared on several examples with that of the displacement-safe scheme of subsection 2.1 and with that of the linear 4-point scheme.

The convexity-preserving scheme is extended in [11] to a co-convexity preserving scheme for general planar polygons. This material is not reviewed here.

3. Quasilinear ENO-based 4-point Interpolatory Schemes

This family of schemes (ENO stands for Essentially Non Oscillatory) was designed to refine scalar data sampled from piecewise smooth functions. In such a scheme

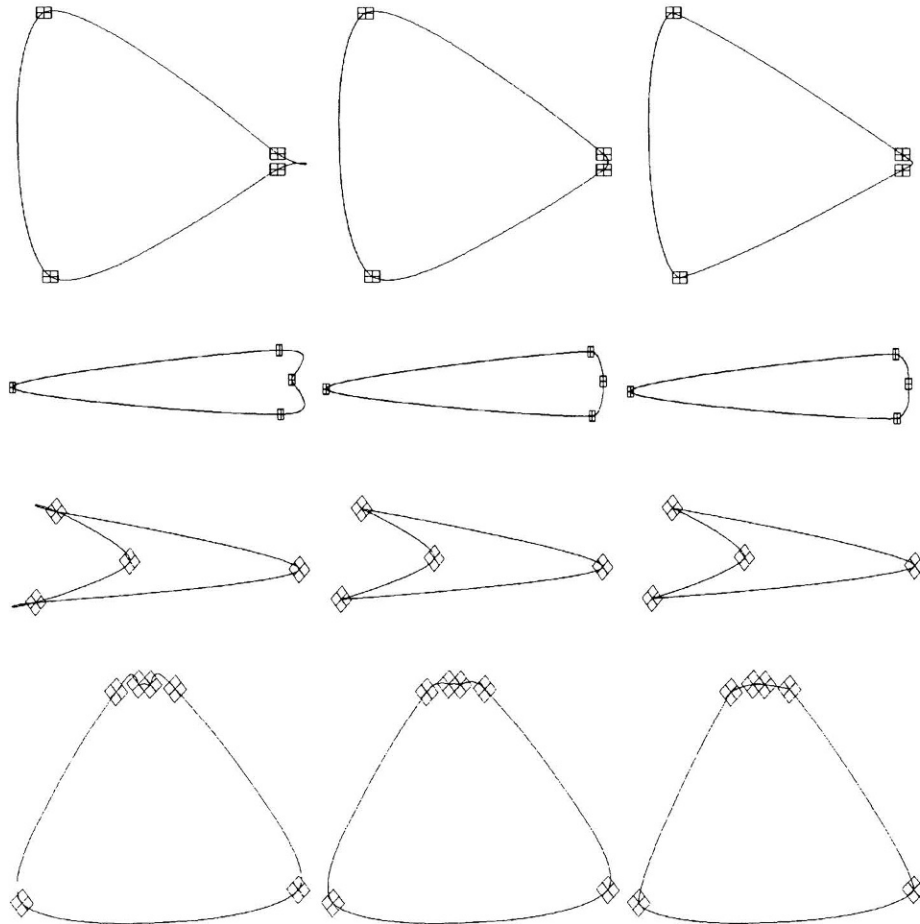


Fig. 4. Examples: (left column) the linear 4-point scheme with $w = 1/16$, (middle column) displacement-safe scheme of (4) with $C = 0.2$, (right column) convexity preserving scheme with $C = 0.9$.

the insertion rules during the refinement process, aim at estimating the function's values in terms of information taken from the same smoothness region. This idea can lead to schemes with quality of approximation similar to that of the linear 4-point scheme with $w = \frac{1}{16}$, when applied to data sampled from smooth functions. In the latter case the values f_j^{k+1} attached to the points $2^{-k-1}j, j \in \mathbb{Z}$, are, in fact, estimated from the values at refinement level k , by

$$f_{2j}^{k+1} = f_j^k, \quad f_{2j+1}^{k+1} = Q_{k,j}^c(2^{-(k+1)}(2j+1)), \quad j \in \mathbb{Z},$$

with $Q_{k,j}^c$, a cubic polynomial satisfying

$$Q_{k,j}^c(2^{-k}(j+i)) = f_{j+i}^k, \quad i = -1, 0, 1, 2. \quad (6)$$

By the ENO approach, we can use two other interpolating polynomials. One is a cubic polynomial interpolating the data in the two endpoints of the interval

$2^{-k}(j, j+1)$, and in two points to its left. This is called a left stencil, and the interpolating cubic polynomial, $Q_{k,j}^\ell$ satisfies

$$Q_{k,j}^\ell(2^{-k}((j+i))) = f_{j+i}^k, \quad i = -2, -1, 0, 1. \quad (7)$$

The other polynomial is the cubic polynomial satisfying

$$Q_{k,j}^r(2^{-k}(j+i)) = f_{j+i}^k, \quad i = 0, 1, 2, 3. \quad (8)$$

The polynomial in (6) is based on a central stencil and that in (8) on a right stencil. The three different estimations for f_{2j+1}^{k+1} resulting from (7), (6) and (8) evaluated at $2^{-(k+1)}(2j+1)$, are

$$\begin{aligned} f_{2j+1}^{k+1,\ell} &= \frac{1}{16}f_{j-2}^k - \frac{5}{16}f_{j-1}^k + \frac{15}{16}f_j^k + \frac{5}{16}f_{j+1}^k \\ f_{2j+1}^{k+1,c} &= \frac{1}{16}f_{j-1}^k + \frac{9}{16}f_j^k + \frac{9}{16}f_{j+1}^k - \frac{1}{16}f_{j+2}^k \\ f_{2j+1}^{k+1,r} &= \frac{5}{16}f_j^k + \frac{15}{16}f_{j+1}^k - \frac{5}{16}f_{j+2}^k + \frac{1}{16}f_{j+3}^k \end{aligned}$$

The selection of the stencil for the estimation of f_{2j+1}^{k+1} is data dependent. It follows the idea of Harten, Enquist, Osher and Chakravarty [9], that in the vicinity of a singularity in the smoothness, data taken from the same smoothness region of the function yields better estimates, and that such data is less oscillatory than data taken from the two sides of the singularity point. An example of a selection mechanism of a stencil is the choice of the “least oscillatory” interpolating polynomial, namely among $Q_{k,j}^\ell, Q_{k,j}^c, Q_{k,j}^r$ the one with least L_2 -norm over the interval $2^{-k}(j, j+1)$.

The resulting ENO-based interpolatory subdivision scheme, converges for any initial data to a Hölder continuous limit function with exponent at least 0.66, and has the important property that if the initial data is sampled from a cubic polynomial, the limit function is that cubic polynomial.

The convergence of the ENO-based scheme, and its property of reproduction of cubic polynomials, guarantee that the limit function generated from the data $f(ih)$, $i \in \mathbb{Z}$, approximates, when scaled properly, the function f , at the rate $O(h^4)$, provided that f is smooth.

Since the selection mechanism does not guarantee that the selected stencil is indeed contained in the same smoothness region, it is not clear how to extend the above approximation result to piecewise smooth functions. For an analysis of a related approximation operator based on the ENO idea, see [1].

The application of a subdivision scheme in a multiscale decomposition and reconstruction with thresholding (e.g. for compression), requires the scheme to be stable, in the sense that small changes in the data result in small changes in the limit function. Converging linear schemes are stable, but the ENO-based 4-point scheme is not, because the selection mechanism is not continuous in the data.

To obtain a stable scheme, the ENO selection mechanism is replaced by the WENO selection mechanism (Weighted ENO), which is continuous in the data on the one hand, and retains the ENO idea on the other hand. In this scheme

$$f_{2j}^{k+1} = f_j^k, \quad f_{2j+1}^{k+1} = Q_{k,j}^w(2^{-(k+1)}(2j+1)),$$

where $Q_{k,j}^w$ is a convex combination of $Q_{k,j}^r, Q_{k,j}^c, Q_{k,j}^\ell$ with coefficients $\alpha_0, \alpha_1, \alpha_2$ respectively.

There are various possible choices of $\alpha_0, \alpha_1, \alpha_2$ as continuous functions of the data $f_{j-2}^k, f_{j-1}^k, \dots, f_{j+3}^k$. The idea of WENO is developed in [3], where an explicit choice is suggested. In this choice, the weights attached to stencils containing a singularity are small.

With the above suggested selection mechanism of the weights, the resulting subdivision scheme converges to Hölder continuous limit functions with exponent bounded below by 0.66. The scheme is C^s -stable for $s \leq 0.66$, namely for $u, v \in \ell_\infty(\mathbb{Z})$, and with $S^\infty(u)$ denoting the limit function generated by the scheme from the initial data u ,

$$\|S^\infty(u) - S^\infty(v)\|_{C^s} \leq C\|u - v\|_{\ell_\infty},$$

where the constant C depends in a non-decreasing way on $\max\{\|v\|_{\ell_\infty}, \|u\|_{\ell_\infty}\}$, and where

$$\|f\|_{C^s} = \sup_{x,y} \left| \frac{f(x) - f(y)}{(x-y)^s} \right|.$$

The method of analysis of convergence and smoothness in [2] is an extension of the method in the linear case, which is based on the scheme for the differences [6]. The reproduction of low degree polynomials and the locality of the investigated schemes, are central to the analysis. In the stability analysis, the existence of a restriction operator from a fine level back to the coarser level is used. The theory is developed for the class of quasi-linear schemes, defined in terms of a data dependent subdivision operator S , which is applied repeatedly. S associates with each $v \in \ell_\infty(\mathbb{Z})$ a linear operator $S(v) : \ell_\infty(\mathbb{Z}) \rightarrow \ell_\infty(\mathbb{Z})$ of the form

$$(S(v)w)_k = \sum_\ell a_{k,\ell}(v)w_\ell$$

with $a_{k,\ell}(v) = 0$ if $|k - 2\ell| > M$, for some $M > 0$ independent of v . The values generated by the quasi-linear subdivision scheme at refinement level k are

$$f^k = S(f^{k-1}) \cdots S(f^1)S(f^0)f^0, \quad k = 1, 2, \dots$$

The general theory for quasi-linear schemes, developed in [2], is applied there to the special case of $2N$ -point ENO-based and WENO-based schemes.

4. Curve Subdivision Schemes on Manifolds

Linear subdivision schemes for curves refine control polygons in 3D or 2D. Starting from an initial control polygon $\mathcal{P}^0 = \{P_i^0\}$, which is the polygonal line through the control points $\{P_i^0\}$, and refining repeatedly, a linear subdivision scheme S generates a sequence of control polygons

$$S^\ell \mathcal{P}^0, \quad \ell = 1, 2, \dots$$

To design subdivision schemes for curves on a manifold, we require that the control points generated at each refinement level are on the manifold, and that the limit of the sequence of corresponding control polygons is on the manifold. Such schemes are nonlinear. Here we discuss two constructions of subdivision schemes on manifolds from converging linear schemes. Both constructions rely on the observation that any converging linear scheme can be calculated by repeated binary averages.

4.1. Converging linear schemes by repeated binary averages

A linear scheme for curves, S , is defined by two refinement rules of the form,

$$P_j^{k+1} = \sum_i a_{j-2i} P_i^k, \quad j = 0 \text{ or } 1(\text{mod } 2). \quad (9)$$

Any converging linear scheme is affine invariant, namely $\sum_i a_{j-2i} = 1$ (see e.g.[6]). As is shown in [17], for a converging linear scheme, each of the refinement rules in (9) is expressible, in a non-unique way, by repeated binary averages. A reasonable choice is a symmetric representation relative to the topological relations in the control polygon.

For example the 4-point scheme (1) can be rewritten as

$$P_{2j}^{k+1} = P_j^k, \quad P_{2j+1}^{k+1} = Av_{\frac{1}{2}}(Av_{(-2w)}(P_j^k, P_{j-1}^k), Av_{(-2w)}(P_{j+1}^k, P_{j+2}^k)),$$

where $Av_\alpha(P, Q) = (1 - \alpha)P + \alpha Q$, $\alpha \in \mathbb{R}$, $P, Q \in \mathbb{R}^n$. Refinement rules represented in this way are termed hereafter “refinement rules in terms of repeated binary averages”.

Among the linear schemes there is a class of “factorizable schemes” for which the symbol $a(z) = \sum_i a_i z^i$, can be written as a product of linear real factors. For such a scheme, the control polygon obtained by one refinement step of the form (9), can be achieved by several simple global steps, uniquely determined by the factors of the symbol.

To be more specific, let us consider a symbol of the form

$$a(z) = z^{-\nu}(1+z)^{\frac{1+x_1z}{1+x_1}} \cdots \frac{1+x_mz}{1+x_m}, \quad (10)$$

with ν a positive integer. Note that this symbol corresponds to an affine invariant scheme since $a(1) = 2$, and $a(-1) = 0$, and that the symbol of any affine invariant scheme has the factor $1+z$, and satisfy $a(1) = 2$. Thus the form of the symbol in (10) is general for converging factorizable schemes.

Let $\{P_i^k\}$ denote the control points at refinement level k . The first step in calculating the control points at level $k+1$ corresponds to the factor $1+z$, and consists of splitting,

$$P_{2i}^{k+1,0} = P_{2i+1}^{k+1,0} = P_i^k. \quad (11)$$

This step is followed by m averaging steps corresponding to the factors $\frac{1+x_jz}{1+x_j}$:

$$P_i^{k+1,j} = \frac{1}{1+x_j}(P_i^{k+1,j-1} + x_j P_{i-1}^{k+1,j-1}), \quad j = 1, \dots, m. \quad (12)$$

Due to the factor $z^{-\nu}$, the control points at level $k+1$ are $P_i^{k+1} = P_{i+\nu}^{k+1,m}$. We term this procedure “global refinement procedure by repeated averaging”.

Note that the symbol of a symmetric scheme ($a_{-j} = a_j$) has even m , $\nu = \frac{m}{2}$ and $x_j^{-1} = x_{m+1-j}$, $j = 1, \dots, \frac{m}{2}$.

A very well known family of factorizable schemes are the B-spline schemes. The symbol of a scheme generating spline curves of order $m+1$ (of degree m) is

$$a(z) = (1+z)^{m+1}/2^m.$$

The 4-point scheme (1) is a symmetric scheme. With $w = \frac{1}{16}$ it is also factorizable. Its symbol has the form

$$a(z) = z^{-3}(1+z) \left(\frac{1+z}{2}\right)^3 \frac{1-(2-\sqrt{3})z}{\sqrt{3}-1} \cdot \frac{1-(2+\sqrt{3})z}{-(\sqrt{3}+1)}.$$

4.2. Construction of subdivision schemes on manifolds

The construction of nonlinear schemes on manifolds starts from a converging linear scheme, S , given either by local refinement rules in terms of repeated binary averages, or given by a global refinement procedure in terms of repeated binary averages. The second representation is preferred, if it exists.

The first construction of a subdivision T on a manifold M , “analogous to S ”, replaces every binary average in the representation of S , by a corresponding geodesic average on M . Thus $Av_\alpha(P, Q)$ is replaced by $gAv_\alpha(P, Q)$, where $gAv_\alpha(P, Q) = c(\alpha\tau)$, with $c(t)$ the geodesic curve on M from P to Q , satisfying $c(0) = P$ and $c(\tau) = Q$. The resulting subdivision scheme is termed geodesic subdivision scheme.

The second construction uses a smooth projection mapping onto M , and replaces every binary average by its projection onto M . The resulting nonlinear scheme is termed a projection subdivision scheme. One possible choice of the projection mapping is the orthogonal projection onto the manifold.

Example 2. In this example the linear scheme is the Chaikin algorithm ,

$$P_{2j}^{k+1} = Av_{\frac{1}{4}}(P_j^k, P_{j+1}^k), \quad P_{2j+1}^{k+1} = Av_{\frac{3}{4}}(P_j^k, P_{j+1}^k), \quad (13)$$

with the symbol $a(z) = (1+z)^3/4$.

Chaikin algorithm, calculated by a global procedure in terms of repeated binary averages:

$$P_{2i}^{k+1,0} = P_{2i+1}^{k+1,0} = P_i^k, \quad P_i^{k+1,j} = \frac{1}{2}(P_i^{k+1,j-1} + P_{i-1}^{k+1,j-1}), \quad j = 1, 2. \quad (14)$$

Chaikin geodesic scheme, derived from (13):

$$P_{2j}^{k+1} = gAv_{\frac{1}{4}}(P_j^k, P_{j+1}^k), \quad P_{2j+1}^{k+1} = gAv_{\frac{3}{4}}(P_j^k, P_{j+1}^k).$$

Chaikin geodesic scheme, derived from (14):

$$P_{2i}^{k+1,0} = P_{2i+1}^{k+1,0} = P_i^k, \quad P_i^{k+1,j} = gAv_{\frac{1}{2}}(P_i^{k+1,j-1}, P_{i-1}^{k+1,j-1}), \quad j = 1, 2.$$

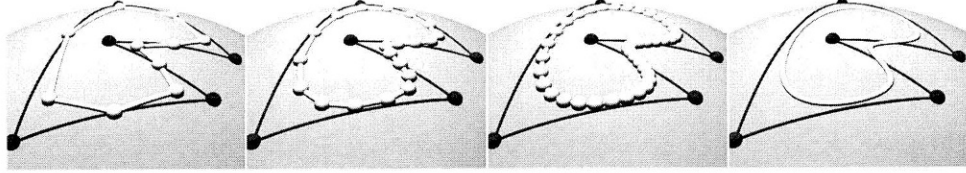


Fig. 5. Geodesic B-Spline subdivision of degree three. From left to right: Tp , $T^2 p$, $T^3 p$, $T^\infty p$.

Chaikin projection scheme derived from (13):

$$P_{2j}^{k+1} = G(Av_{\frac{1}{4}}(P_j^k, P_{j+1}^k)), \quad P_{2j+1}^{k+1} = G(Av_{\frac{3}{4}}(P_j^k, P_{j+1}^k)).$$

Chaikin projection scheme derive from (14):

$$P_{2i}^{k+1,0} = P_{2i+1}^{k+1,0} = P_i^k, \quad P_i^{k+1,j} = G(Av_{\frac{1}{2}}(P_i^{k+1,j-1}, P_{i-1}^{k+1,j-1})), \quad j = 1, 2.$$

In the above G is a specific projection mapping on the manifold M .

Figure 5 displays a curve on a sphere, created by a geodesic analogous scheme to a third degree B-spline scheme, from a finite number of initial control points on the sphere.

4.3. Analysis of convergence and smoothness

The analysis of convergence and smoothness of the geodesic and the projection schemes is based on their proximity to the linear scheme from which they are derived, and on the smoothness properties of this linear scheme. This method of proof works for at most C^2 smoothness. To formulate the proximity conditions we introduce some notation.

For a control polygon $\mathcal{P} = \{P_i\}$, we define $\Delta^0 \mathcal{P} = \mathcal{P}$, $\Delta \mathcal{P} = \{P_{i+1} - P_i\}$, and

$$\Delta^{\ell+1} \mathcal{P} = \Delta(\Delta^\ell \mathcal{P}), \quad d_\ell(\mathcal{P}) = \max_i \|(\Delta^\ell \mathcal{P})_i\|, \quad \ell = 0, 1, \dots$$

The difference between two control polygons $\mathcal{P} = \{P_i\}$, $\mathcal{Q} = \{Q_i\}$, is defined as $\mathcal{P} - \mathcal{Q} = \{P_i - Q_i\}$.

With this notation the two proximity relations of interest to us are the following. Here, C is a generic constant.

Definition 3.

(i) Two schemes S and T are in 0-proximity if

$$d_0(S\mathcal{P} - T\mathcal{P}) \leq C d_1(\mathcal{P})^2$$

for all control polygons \mathcal{P} with $d_1(\mathcal{P})$ small enough.

(ii) Two schemes S and T are in 1-proximity if

$$d_1(S\mathcal{P} - T\mathcal{P}) \leq C[d_1(\mathcal{P})d_2(\mathcal{P}) - d_1(\mathcal{P})^3].$$

for all control polygons \mathcal{P} with $d_1(\mathcal{P})$ small enough.

We can deduce the convergence of T from the convergence of a linear scheme S , if S and T satisfy the 0-proximity condition. Under certain conditions on S , we can also deduce that T generates C^1 limit curves.

Theorem 4. *Let S be a convergent linear subdivision scheme, and let T and S be in 0-proximity. Then the sequence of control polygons $\{T^\ell \mathcal{P}\}_\ell$ for \mathcal{P} , with $d_1(\mathcal{P})$ small enough, converges in the sup-norm to a continuous curve.*

Moreover, if S generates C^1 limit curves and satisfies, for all \mathcal{P} , that $d_1(S^L \mathcal{P}) \leq \mu d_1(\mathcal{P})$ for some $L \in \mathbb{Z}_+$ and $\mu \leq (\frac{1}{2})^{\frac{L}{2}}$, then the limit of $\{T^\ell \mathcal{P}\}$ is a C^1 curve whenever such a limit exists.

Results on C^2 smoothness of T require also the 1-proximity condition [18].

Theorem 5. *Let S and T be in 0-proximity and in 1-proximity. If S is a linear scheme satisfying for all control polygons \mathcal{P} ,*

$$d_j(2^{L(j-1)} S^L \mathcal{P}) \leq \mu_j d_j(\mathcal{P}), \quad j = 1, 2, 3, \quad (15)$$

for some $L \in \mathbb{Z}_+$, and with μ_i , $i = 1, 2, 3$, satisfying

$$\mu_i < \mu_i^* \leq 1, \quad i = 1, 2, 3, \quad (16)$$

$$\mu_3^* = 1, \quad \mu_1^{*2} \leq \frac{\mu_2^*}{2^L}, \quad \mu_1^{*3} \leq \frac{1}{2^{2L}}, \quad \mu_1^* \mu_2^* \leq \frac{1}{2^{2L}}, \quad (17)$$

then the curves generated by T are C^2 .

It should be noted that a linear scheme S , generates C^2 limit curves if it satisfies equation(15) with $0 < \mu_i < 1$ for $i = 1, 2, 3$ (see e.g. [6]). Yet, the proof in [18] that the proximity relations between S and T imply that T also generates C^2 curves, is valid only for a restricted class of linear schemes satisfying equation (15) under the restrictions of (16) and (17).

The following theorem gives conditions for a nonlinear scheme T , generating curves on a manifold, and a converging linear scheme S , to satisfy the proximity conditions of Definition 3.

Theorem 6. *Let T be a geodesic or a projection subdivision scheme on a smooth manifold M , derived from a converging linear scheme S . Then S and T satisfy the two proximity conditions of Definition 3. In case M is a compact manifold or a surface with bounded normal curvatures, there exists a global $\delta > 0$, such that the proximity conditions hold for all \mathcal{P} satisfying $d_1(\mathcal{P}) < \delta$.*

Example 7. It is well known that a factorizable linear scheme S , generating C^2 curves, has at least three of the $\{x_i\}$ in (10) equal to 1. Since for B-spline schemes $L = 1$ and $\mu_i = \frac{1}{2}$ in (15), it follows from the last two theorems that the geodesic

and the projection analogous schemes of the B-spline schemes of degree ≥ 3 generate C^2 curves.

The linear 4-point scheme with $w = \frac{1}{16}$ is only C^1 and not C^2 , although its symbol has the factor $(1+z)^4$. Therefore its nonlinear analogous schemes are not C^2 , as the conditions of Theorem 5 are not satisfied.

References

1. Arandiga, P., Cohen, A., Donat, R. and Dyn, N., Interpolation of piecewise smooth functions, *Applied Comp. Harmonic Analysis*, to appear.
2. Cohen, A., Dyn, N. and Matei, B., Quasilinear subdivision schemes with applications to ENO interpolation, *Applied Comp. Harmonic Analysis* **15** (2003), 89–116.
3. Chang, T., Liu, X.-D. and Osher, S., Weighted essentially non-oscillatory schemes, *J. Comput. Phys.* **115** (1994), 200–212.
4. Daubechies, I., *Ten Lectures on Wavelets*, SIAM, Philadelphia, 1992.
5. Daubechies, I., Runborg, O. and Sweldens, W., Normal multiresolution approximation of curves, *Constr. Approximation* **20** (2004), 399–463.
6. Dyn, N., Subdivision schemes in Computer-Aided Geometric Design, in: *Advances in Numerical Analysis - Vol. II, Wavelets, Subdivision Algorithms and Radial Basis Functions* (W. Light, Ed.), Clarendon Press, Oxford, 1992, pp. 36–104.
7. Dyn, N. and Levin, D., Analysis of asymptotically equivalent binary subdivision schemes, *J. Math. Analysis and Applications* **193** (1995), 594–621.
8. Dyn, N., Gregory, J. and Levin, D., A 4-point interpolatory subdivision scheme for curve design, *Computer Aided Geometric Design* **4** (1987), 257–268.
9. Harten, A., Enquist, B., Osher, S. and Chakravarty, S., Uniformly high order accurate essentially non-oscillatory schemes III, *J. Comput. Phys.* **71** (1987), 231–303.
10. Levin, D., Using Laurent polynomial representation for the analysis of the non-uniform binary subdivision schemes, *Advances in Computational Mathematics* **11** (1999), 41–54.
11. Marinov, M., Dyn, N. and Levin, D., Geometrically controlled 4-point interpolatory schemes, in: *Advances in Multiresolution for Geometric Modelling* (N. A. Dodgson, M. S. Floater and M. A. Sabin, Eds.), Springer-Verlag, New York, 2005.
12. Noaks, L., Nonlinear corner cutting, *Advances in Computational Mathematics* **8** (1998), 165–177.
13. Noaks, L., Accelerations of Riemannian quadratures, *Proc. Amer. Math. Soc.* **127** (1999), 1827–1836.
14. Oswald, P., Smoothness of nonlinear subdivision schemes, in: *Curve and Surface Fitting*, Proc. Saint-Malo 2002, (A. Cohen, J.-L. Merrien and L. L. Schumaker, Eds.), Nashboro Press, Brentwood, 2003, pp. 323–332.

15. Rahman, I. U., Drori, I., Stodden, V., Donoho, D. L. and Schroeder, P., Multiscale representations for manifold-valued data, preprint.
16. Sabin, M., A circle-preserving variant of the four-point subdivision scheme, preprint.
17. Wallner, J. and Dyn, N., Convergence and C^1 analysis of subdivision schemes on manifolds by proximity, *Computer Aided Geometric Design*, to appear.
18. Wallner, J., Smoothness analysis of subdivision schemes by proximity, preprint.
19. Xie, G. and Yu, T. P.-Y., On a linearization principle for nonlinear p -mean subdivision schemes, in: *Advances in Constructive Approximation* (M. Neamtu and E. B. Saff, Eds.), Nashboro Press, Brentwood, 2004, pp. 519–533.
20. Xie, G. and Yu, T. P.-Y., Smoothness analysis of nonlinear subdivision schemes of homogeneous and affine invariant type, *Constr. Approximation*, to appear.